

Trapped-hole defects in SrO[†]

J. Rubio O.,* H. T. Tohver,[‡] Y. Chen, and M. M. Abraham

Solid State Division, Oak Ridge National Laboratory, Oak Ridge, Tennessee 37830

(Received 3 September 1976)

We report the successful production of V^- and V^0 defects in SrO. Since hydrogen has been found to be necessary for V^- formation in MgO, SrO single crystals were intentionally doped with hydrogen during growth. Both these defects were detected after a short γ irradiation at 77 K in crystals previously irradiated with high doses of either neutrons, electrons, or γ rays. Electron-paramagnetic-resonance (EPR) measurements showed that the V^- center exhibits $\langle 100 \rangle$ axial symmetry at 77 K characterized by $g_{\parallel} = 2.0013(2)$ and $g_{\perp} = 2.0705(2)$. At 270 K, the EPR spectrum consists of a single thermally-averaged isotropic line at $g = 2.047(1)$. An extensive electron-nuclear double-resonance search at 4.2 K revealed no charge-compensating impurities associated with this center. The V^0 center also displays $\langle 100 \rangle$ axial symmetry at 77 K with the following parameters: $S = 1$, $g_{\parallel} = 2.0012(2)$, $g_{\perp} = 2.0748(2)$, and $D = 127.05(5) \times 10^{-4} \text{ cm}^{-1}$. The absence of V^0 signals at 4.2 K established that the $S = 1$ triplet state is an excited state. At ~ 210 K, the V^0 centers begin to decay into the more stable V^- center. The latter has a room-temperature half-life of ~ 25 min. Additional defects are also reported. In particular an $S = 1/2$ axial center is tentatively identified as an $(\text{OF})^{2-}$ molecular ion oriented along $\langle 111 \rangle$ directions.

INTRODUCTION

Positive-ion vacancies in the alkaline-earth oxides, both intrinsic and impurity compensated, have been of immense interest since their identification many years ago.¹ Recently, some fundamental aspects of the formation mechanism in MgO for the intrinsic V^- and V^0 defects (positive-ion vacancy with one and two trapped holes, respectively) have been elucidated.^{2,3} While the paramagnetic V^- center has been identified unequivocally in MgO and CaO,²⁻⁸ its existence in SrO has been somewhat questionable since centers with different parameters have been proposed as being the V^- center.

Culvahouse, Holroyd, and Kolopus,⁹ while studying the F^+ center in neutron-irradiated SrO single crystals, observed an extra center in the (EPR) electron-paramagnetic-resonance spectrum which exhibited $\langle 100 \rangle$ axial symmetry with $g_{\parallel} = 2.0010(6)$ and $g_{\perp} = 2.0703(6)$. They suggested that it might be the V^- center. At about the same time, Suss found a defect characterized by $g_{\parallel} = 1.9999$ and $g_{\perp} = 2.0757$, which he also proposed to be the V^- center.¹⁰ The reported defects in both investigations were thermally unstable at room temperature. In neither case were any $S = 1$, V^0 centers observed.

Recently, Tench and Duck¹¹ studied proton-irradiated SrO powders at 77 K and observed an EPR signal at $g_{\perp} = 2.0667(1)$ which had a half-life of 5 min at 295 K. They attributed this signal to the V^- center. These authors also observed an $S = 1$ defect characterized by $g_{\perp} = 2.0713(1)$ and $D = 123 \times 10^{-4} \text{ cm}^{-1}$, which they proposed to be the V^0 cen-

ter. No parallel g values were reported for either center.

It has been conclusively shown that, for MgO, the production of V^- centers depends on the presence of hydrogen in the crystal.^{2,3} Assuming a similar mechanism in SrO, we grew SrO crystals with intentional hydrogen doping. (The same technique has been used successfully to produce V^- centers in CaO.⁸)

In this paper, we report the successful production and identification of V^- and V^0 centers in hydrogenated SrO single crystals. The V^- center exhibits an axial EPR spectrum at 77 K with a set of g values which are different from those reported by Suss¹⁰ and by Tench and Duck.¹¹ On the other hand, our results for this center are in agreement with those reported by Culvahouse *et al.*⁹ within the quoted errors. However, past experience has emphasized the danger in identifying a defect from its numerical g values alone.^{4,12} Our evidence for identifying this defect as the V^- center can be stated as follows. (a) No charge-compensating impurities could be detected using electron-nuclear double-resonance (ENDOR) techniques. (b) The EPR transitions seen at 77 K thermally average, producing a single isotropic line at 270 K. (c) The production of $S = 1$, V^0 centers and their subsequent conversion to V^- centers upon annealing. (d) The relatively high stability of this defect which is compatible with a positive hole trapped by a negatively charged defect.

The spin-Hamiltonian parameters obtained for the V^0 center in the single crystal are different from those previously published for the powder.¹¹ From the angular variations of the EPR spectra, the axial symmetry of both centers is definitely

established. Additional low-symmetry defects are also reported for the first time in SrO.

EXPERIMENTAL PROCEDURES

The SrO single crystals used in the present investigation were grown in this laboratory from SrCO_3 powders using the arc-fusion technique.¹³ The starting materials were from two sources: Mallinckrodt Chemical Company and Sherwin-Williams Company. Crystals grown with powders from these two sources will be designated SrO (M) and SrO (SW), respectively. They were intentionally doped with hydrogen by the absorption of water vapor and then regrown. No effort was made to establish the absolute concentration of hydrogen in these crystals, but its presence was revealed in the form of V_{OH} centers in crystals given small doses of γ rays. As in MgO ,^{2,3} prolonged irradiation reduced the V_{OH} concentration and increased that of the V^\cdot . Apart from hydrogen, manganese was detected by EPR measurements in SrO (M) crystals and a much lower concentration was found in the SrO (SW) crystals. The powder from the latter source, however, contained much larger concentrations of barium and calcium impurities (~ 1000 ppm).

The positive-ion vacancies were produced by neutron, electron, and long-period γ irradiations. Neutron irradiations were carried out in the Bulk-Shielding Reactor at Oak Ridge National Laboratory to doses of $\sim 10^{18}$ n/cm². Electron irradiations were performed at ~ 300 K with 2.0 MeV electrons from a Van de Graaff generator to $\sim 10^{17}$ e/cm². Since γ irradiation is not nearly as efficient as electrons in producing Sr vacancies in the crystals, SrO crystals were also irradiated in a ^{137}Cs γ source for one month. In order to trap the holes next to the Sr vacancies, a 30-min γ irradiation at 77 K prior to measurement was required with the sample subsequently transferred to the resonance spectrometer without appreciable intervening warmup. Measurements at 100 K were done with a conventional X-band homodyne spectrometer while at 77 K and liquid helium temperatures, measurements were performed on an X-band superheterodyne spectrometer with ENDOR capabilities. Magnetic fields were measured with a proton-nuclear resonance probe. A Hewlett-Packard 5245L frequency counter with a model 5255A frequency converter was employed to measure both the proton and the electron resonance frequencies.

RESULTS AND DISCUSSION

Examination of a neutron-irradiated SrO (SW) crystal showed the isotropic single-line spectrum of the F^\cdot center ($g = 1.9845$) with resolved hyper-

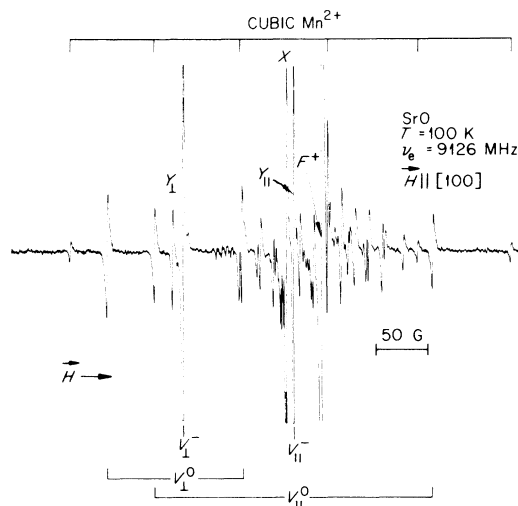


FIG. 1. EPR absorption spectrum of a neutron-irradiated SrO crystal followed by γ irradiation at 77 K.

fine structure due to centers with one and two nearest-neighbor ^{87}Sr nuclei as the most prominent feature.⁹ Weak cubic Mn^{2+} hyperfine lines corresponding to the $M_s = +\frac{1}{2} \rightarrow M_s = -\frac{1}{2}$ transition were also detected. Immediately after γ irradiation at 77 K, this crystal shows the paramagnetic resonance spectrum illustrated in Fig. 1 with $\vec{H} \parallel [100]$.

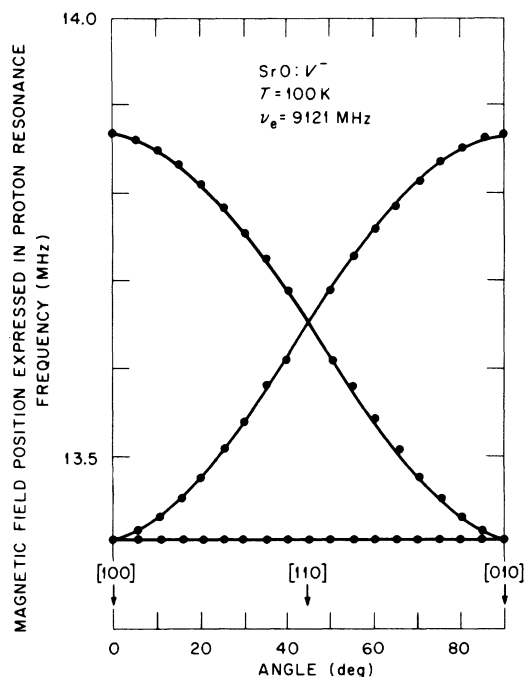


FIG. 2. EPR angular variation in the (001) plane for the $\text{SrO}:V^\cdot$ center. Experimental points are compared with the theoretical curves obtained from the principal g values.

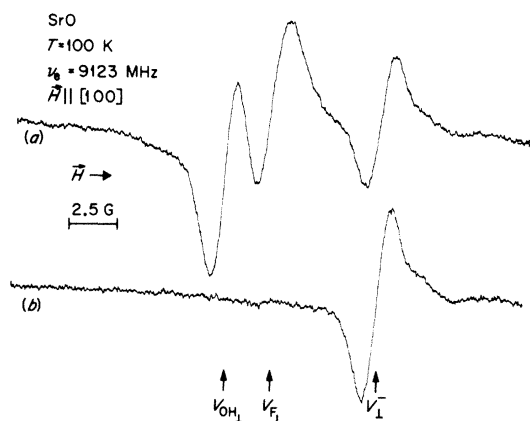


FIG. 3. EPR spectra of trapped hole centers in an electron-irradiated SrO crystal with \vec{H} perpendicular to the principal axis. Following (a) γ irradiation at 77 K and (b) a subsequent anneal at 295 K for 1.5 min.

With the exception of the F^+ center and two other defects X and Y , which will be discussed later, the V^- and V^0 centers were the most prominent defects. The EPR angular variation of the V^- center for magnetic-field orientations in the (001) plane is illustrated in Fig. 2. This angular variation is char-

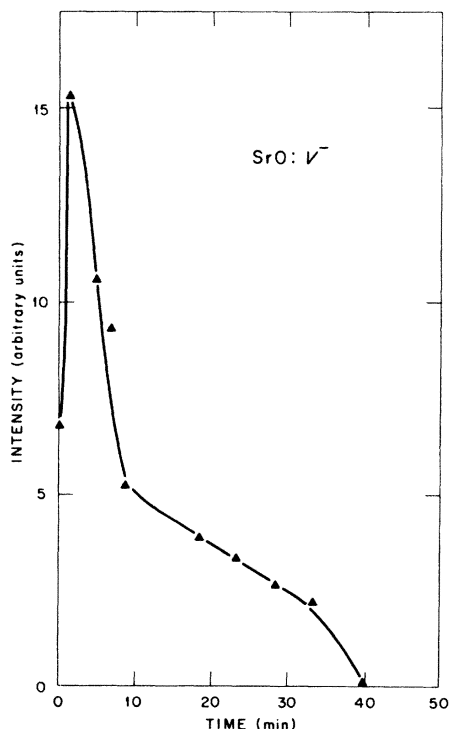


FIG. 4. Thermal stability of the V^- center in SrO single crystals at 295 K.

acteristic of an $S = \frac{1}{2}$ center with axial symmetry described by the spin Hamiltonian:

$$\mathcal{H} = \mu_B [g_{\parallel} H_z S_z + g_{\perp} (H_x S_x + H_y S_y)]. \quad (1)$$

The principal axes of the g tensor lie along $\langle 100 \rangle$ crystallographic directions with the following values: $g_{\parallel} = 2.0013(2)$ and $g_{\perp} = 2.0705(2)$. Figure 3 shows a high-resolution EPR spectrum after γ irradiation at 77 K of a previously electron-irradiated SrO (M) crystal with the magnetic field applied perpendicular to the principal symmetry axis. In this case, besides the V^- and V^0 centers, the V_{OH} and V_F defects were also produced by the γ irradiation. The latter two centers were verified by ENDOR to be associated with hydrogen and fluorine, respectively.¹² The field positions of the EPR lines for the V^- , V_{OH} , and V_F centers in SrO are in the same sequence as in MgO and CaO.^{3,8,14} Annealing of the crystal in air at 295 K for ~ 1.5 min destroys the V^0 , V_{OH} , and V_F EPR resonances while enhancing the V^- signal as revealed by a subsequent low-temperature measurement. At 77 K, the widths of the V^- EPR lines are ~ 0.6 G. On warming the sample from 77 K, the EPR V^- lines broaden and merge to form a well-resolved isotropic line (at 270 K linewidth ~ 16 G) with a g value of 2.047(1). This isotropic g value compares very well with the average value of the low-temperature axial values $\frac{1}{3}(g_{\parallel} + 2g_{\perp}) = 2.0474$. At low temperature, the axial symmetry shows that the

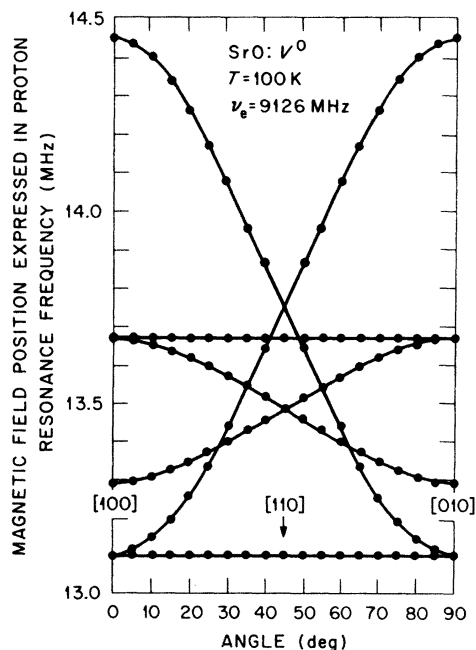


FIG. 5. EPR angular variation in the (001) plane for the V^0 center in SrO. Experimental points are compared with theoretical curves.

hole is preferentially located on one of the neighboring oxygen ions, while the averaging at higher temperatures shows that hole hopping about the six equivalent oxygens takes place. It should be noted that in none of the previous investigations was motional averaging of the g tensor reported.^{9,10,11} To find a possible association with a charge-compensated impurity similar to that discovered in MgO,^{4,15} ENDOR studies were performed on the V^- lines at 4.2 K. No such association could be found and only distant ENDOR responses due to ^{17}O and ^{87}Sr were observed.

In contrast to the MgO and CaO hosts for which the V^- center has been found to be highly stable at room temperature,²⁻⁸ our observed V^- center in SrO has a room-temperature half-life of ~25 min. Figure 4 illustrates its thermal stability. The initial EPR signal intensity of the V^- center was measured at 100 K. The sample was then annealed at room temperature (295 K) for different periods of time with a subsequent measurement of the EPR signal intensity at 100 K after each annealing period.

The EPR spectrum of the V^0 center consists of four lines (Fig. 1) whose angular dependence as \vec{H} is rotated away from the [100] direction in the (001) plane is illustrated in Fig. 5. This angular behavior is characteristic of an axial $S=1$ center described by the spin Hamiltonian:

$$\mathcal{H} = \mu_B [g_{\parallel} H_z S_z + g_{\perp} (H_x S_x + H_y S_y)] + D [S_z^2 - \frac{1}{3} S(S+1)] \quad (2)$$

The principal axes are oriented along the $\langle 100 \rangle$ directions. Values for g_{\parallel} , g_{\perp} , and D were calculated using an iteration procedure correct to second

order in perturbation theory. Results are shown in Table I.

The disappearance of V^0 signals at 4.2 K established that the $S=0$ singlet state is the ground state. A similar situation was found for MgO,³ and CaO.⁸ The linear configuration of the V^0 center is $\text{O}^-(\text{cation vacancy})-\text{O}^-$, and assuming that the fine-structure splitting D is due entirely to a dipole-dipole interaction between the two positive holes, the formula¹⁶

$$hcD = -(2g_{\parallel}^2 + g_{\perp}^2) \mu_B^2 / 2R^3, \quad (3)$$

can be used to calculate the distance R separating the holes, giving $R = 5.95 \text{ \AA}$. Compared to the normal SrO lattice spacing of 5.16 \AA between the oxygens, it implies an outward relaxation of ~15%. A similar calculation for the V^0 center in MgO and CaO, using the data tabulated in Table I, yields values of $R = 4.99$ and 6.16 \AA , respectively.⁸ With normal lattice parameters of 4.21 \AA in MgO and 4.80 \AA in CaO, outward relaxations of ~18 and 28%, respectively, are implied. Such large distortions suggest that Eq. (3) may not be applicable for these systems.

Figure 6 shows isochronal annealing curves for the V^- and V^0 centers in SrO. The results for two different crystals are shown; a neutron-irradiated SrO (SW) crystal (1.4×10^{18} neutrons/cm²) and a SrO (M) sample subjected to room-temperature γ irradiation ($9 \times 10^8 \text{ R}$) for one month. The V^- and V^0 centers were produced simultaneously in these samples by subsequent γ irradiation at 77 K. In both crystals, the V^0 center begins to decay near 210 K while the V^- concentration grows. This process can be represented by $V^0 \rightarrow V^- + \text{hole}$. If this hole from the V^0 center is trapped at a site

TABLE I. Trapped-hole centers in MgO, CaO, and SrO.

Lattice	Defect	g_{\parallel}	g_{\perp}	D (10^{-4} cm^{-1})	Ref. ^a
MgO	V_{OH}	2.0033(2)	2.0398(2)		14
	V_{F}	2.0032(2)	2.0390(2)		14
	V^-	2.0033(2)	2.0386(2)		4
	V^0	2.0033(2)	2.0395(2)	212.61(5) [= 227.33(5) G]	4
CaO	V_{OH}	2.0018(2)	2.0729(2)		14
	V_{F}	2.0017(2)	2.0719(2)		14
	V^-	2.0021(2)	2.0697(2)		7
	V^0	2.0021(2)	2.0733(2)	114.08(5) [= 122.05(5) G]	7
SrO	V_{OH}	2.0014(3)	2.0751(3)		12
	V_{F}	2.0014(3)	2.0736(3)		12
	V^-	2.0013(2)	2.0705(2)		This work
	V^0	2.0012(2)	2.0748(2)	127.05(5) [= 135.99(5) G]	This work

^aSee these papers and references cited therein.

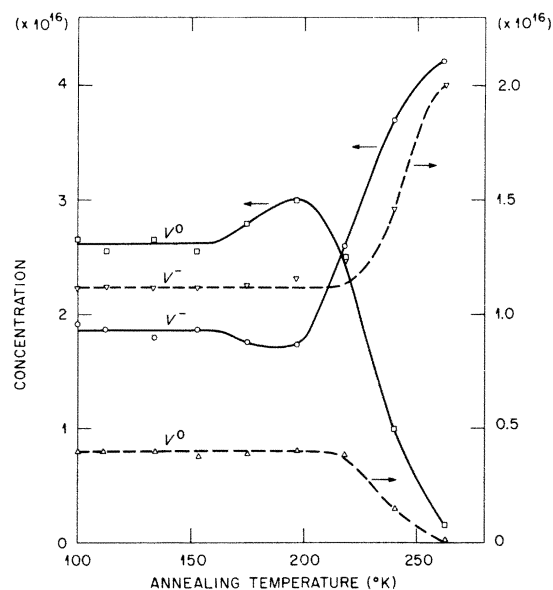


FIG. 6. Concentration of trapped-hole centers in SrO as a function of annealing temperature following γ irradiation at 77 K. Solid line: a crystal previously irradiated with ^{137}Cs γ rays, at room temperature, $\sim 9 \times 10^8$ R. Dashed line: a crystal previously irradiated with $\sim 1.4 \times 10^{18}$ neutrons/cm 2 .

other than a V^{2-} site (cation vacancy), only one V^- center will be formed for every V^0 center, and the sum of the concentrations $V^0 + V^-$ would be conserved. On the other hand, if this hole from the V^0 is relocated at a V^{2-} site, two V^- centers will result from the decay of every V^0 center and the sum $2V^0 + V^-$ would be conserved. Neglecting the release of holes from other traps, a situation bounded between these two extrema is expected. It appears that for the SrO (SW) neutron-irradiated sample, $2V^0 + V^-$ is conserved, while for the SrO (M) crystal, $V^0 + V^-$ is constant. The difference between these two results can be explained in terms of the amount of cation vacancies (V^{2-} centers) produced by the irradiation process. It is expected that neutron irradiation would produce more cation vacancies than the long γ irradiation. Different concentrations of impurities in these two crystals may also produce the difference in the annealing behavior.

Two additional defects X and Y in Fig. 1 were also observed in the neutron-irradiated SrO (SW) crystals. They were detected after γ irradiation at 77 K. The isotropic line X has a linewidth of 0.8 G with $g=2.0062(5)$. The EPR intensity of this line is comparable to that of the F^+ center. This X center is stable at room temperature and no appreciable change in its EPR signal intensity was observed after several weeks. Lines Y are due

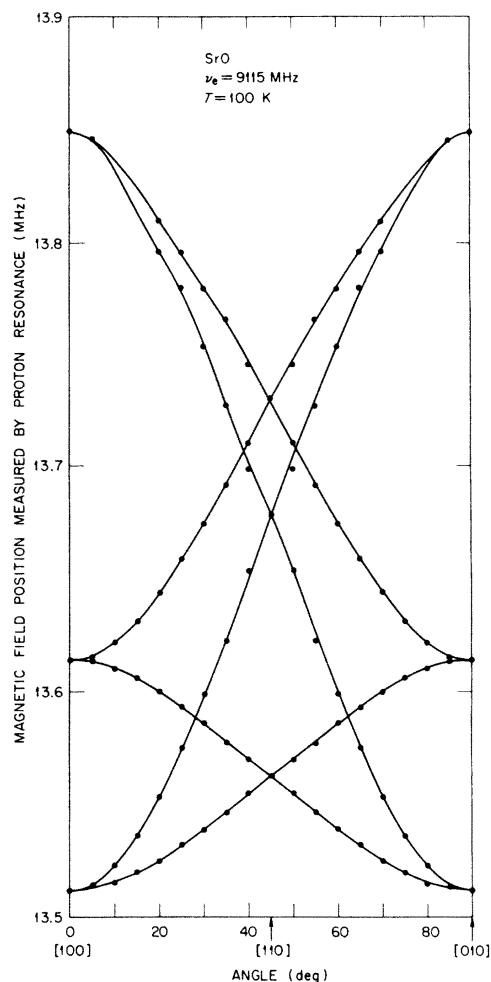


FIG. 7. EPR angular variation in the (001) plane for the orthorhombic defect A in SrO.

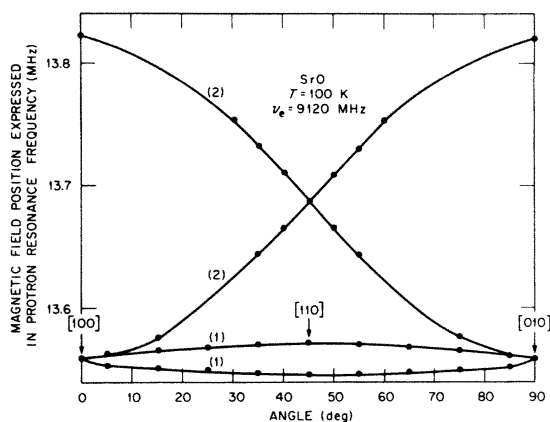


FIG. 8. EPR angular variation in the (001) plane for the orthorhombic B center in SrO. Numbers in parentheses represent the degeneracy of the lines in this particular plane.

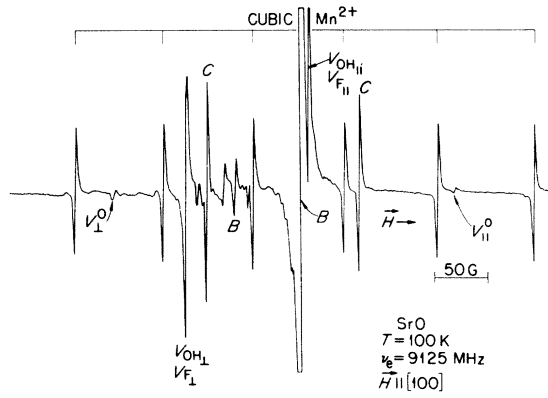


FIG. 9. EPR spectrum of an "as-grown" SrO crystal after γ irradiation at 77 K showing the orthorhombic B center and the trigonal C center. High field line ($\theta = 0^\circ$) for the B center is superimposed on a complex central structure.

to an $S = \frac{1}{2}$ center with $\langle 100 \rangle$ axial symmetry characterized by $g_{\parallel} = 2.0010(3)$ and $g_{\perp} = 2.0769(3)$. This defect is not stable at room temperature and is completely annealed at ~ 270 K. Neither EPR nor ENDOR measurements could detect any impurities associated with the X and Y centers.

In the search for the V^- and V^0 centers, three additional defects A , B , and C were also observed in "as-grown" hydrogenated SrO (M) crystals following γ irradiation at 77 K. Figure 7 shows the EPR angular variation of the orthorhombic defect A for magnetic-field orientations in the (001) plane. The observed spectra were fitted to the orthorhombic spin Hamiltonian:

$$\mathcal{H} = \mu_B (g_x H_x S_x + g_y H_y S_y + g_z H_z S_z), \quad (4)$$

with $S = \frac{1}{2}$ and x , y , and z symmetry axes oriented along $\langle 100 \rangle$ directions. The g values were found to be: $g_x = 2.0514(5)$, $g_y = 2.0362(5)$, and $g_z = 2.0020(5)$. This defect has a room-temperature half-life of ~ 100 min. Figure 8 shows the EPR angular variation for the $S = \frac{1}{2}$ orthorhombic defect B with the magnetic field lying in the (001) plane. In this case, the z axis lies along the $\langle 100 \rangle$ crystalline axes and the x and y axes along the $\langle 110 \rangle$ directions. The observed spectra were fitted to the

spin Hamiltonian [Eq. (4)] and the principal g values were found to be: $g_x = 2.0429(5)$, $g_y = 2.0465(5)$, and $g_z = 2.0063(5)$. The B center is not stable at room temperature and after a short anneal (< 1 min) at 295 K, the EPR lines disappear while the concentration of the defect A is enhanced. Measurements of the EPR signal intensities seem to indicate that B centers decay into more stable A centers upon annealing at room temperature and this may mean that both centers are related. Although several ENDOR attempts were made to detect a possible association of a magnetic nucleus with either the A or B center, none could be discovered.

Finally, Fig. 9 shows the EPR spectrum of the axial paramagnetic defect labeled C , which is unstable at room temperature (half-life < 1 min). It consists of two lines each of which is fourfold degenerate with $\vec{H} \parallel [100]$. By observations of the EPR angular variations in the (100) and (110) planes, it was established that this defect has $\langle 111 \rangle$ axial symmetry, and it was fitted to the spin Hamiltonian:

$$\mathcal{H} = \mu_B [g_{\parallel} H_z S_z + g_{\perp} (H_x S_x + H_y S_y)] + A_{\parallel} S_z I_z + A_{\perp} (S_x I_x + S_y I_y) \quad (5)$$

with $S = \frac{1}{2}$, $I = \frac{1}{2}$. Values for the spin-Hamiltonian parameters were obtained from the data measured with the magnetic field applied along the $\langle 100 \rangle$, $\langle 110 \rangle$, and $\langle 111 \rangle$ directions, using a computer program which makes an exact diagonalization of the energy matrix. With the results given in Table II, the maximum deviation between the computed and the experimental field positions was less than 1 G. It should be noted that the C lines were labeled as A lines in a previous paper.¹² At that time, it was not possible to establish the nature of this center. Defects characterized similarly by $S = \frac{1}{2}$, $I = \frac{1}{2}$ have previously been observed in MgO and CaO. Rius and Cox¹⁷ observed a trigonal $S = \frac{1}{2}$ center in MgO having a large hyperfine interaction with an $I = \frac{1}{2}$ nucleus and a half-life of a few minutes at room temperature. The proposed model was an $(\text{OF})^{2-}$ molecular ion oriented along the $\langle 111 \rangle$ directions. This model was confirmed later by Rius *et al.*¹⁸ by observing the hyperfine interaction of this center

TABLE II. Spin-Hamiltonian parameters for $S = I = \frac{1}{2}$ axial centers.

Host	Defect	Symmetry axes	g_{\parallel}	g_{\perp}	A_{\parallel} (MHz)	A_{\perp} (MHz)	Ref.
CaF ₂	(OF) ²⁻	$\langle 100 \rangle$	2.0016(8)	2.0458(8)	150(1)	43(1)	20
MgO	(OF) ²⁻	$\langle 111 \rangle$	2.0022(2)	2.0085(2)	1273(1)	482(1)	17, 18
CaO	(OH) ²⁻	$\langle 100 \rangle$	2.0067(2)	2.0064(2)	231(3)	153(3)	19
SrO	(OF) ²⁻	$\langle 111 \rangle$	2.0062(2)	2.0206(2)	663(3)	154(3)	This work

with the ^{17}O nucleus in a 10% enriched MgO crystal. Recently, McGeehin *et al.*¹⁹ reported on the investigation of a similar defect in CaO but with $\langle 100 \rangle$ axial symmetry at room temperature and with orthorhombic symmetry at 77 K. These authors proposed the $(\text{OH})^{2-}$ molecular ion as the paramagnetic specie responsible for their observed spectrum, since the hyperfine parameters in CaO were a factor of 5 smaller than those reported for the $(\text{OF})^{2-}$ ion in MgO. They explained the different orientation for the O-H bond as due to the smaller ionic size of the proton compared to the fluorine. Table II shows the reported spin-Hamiltonian parameters for the $(\text{OF})^{2-}$ and $(\text{OH})^{2-}$ ions.¹⁷⁻²⁰ Although either of the two molecular ions $(\text{OH})^{2-}$ and $(\text{OF})^{2-}$ could be responsible for the observed C center in SrO, since both hydrogen and fluorine were detected in the crystal (see Fig. 9), the $(\text{OF})^{2-}$ ion seems to appear as a better candidate in view of its similarity with the MgO center.^{17,18} The other four known elements with 100% natural abundant $I = \frac{1}{2}$ isotopes, which could also produce such a hyperfine splitting in SrO, can be

ruled out by the arguments given by McGeehin *et al.*¹⁹ A definitive model, however, must await ENDOR measurements. Unfortunately at the present time our ENDOR facility does not have the large frequency range required.

CONCLUSION

Our identification of the V^- center in SrO is supported by the motional averaging of the EPR spectrum at high temperatures and the failure of ENDOR to detect any associated impurities. The production of the V^0 center and its observed decay into the V^- center lends further credence to this identification.

Of considerable importance is the fact that we succeeded in producing the V^- center in SrO only in crystals intentionally doped with hydrogen. This has also been true in CaO.⁸ It was demonstrated previously that in MgO,^{2,3} the V_{OH}^- center described by the configuration $\text{OH}^-(\text{Mg vacancy})-\text{O}^{2-}$ is a necessary precursor of the V^- center. We suggest that the same formation mechanism is true in CaO and SrO.

*Permanent address: Instituto de Fisica U. N. A. M., Mexico, D.F.

†Research sponsored by the U.S. ERDA under contract with Union Carbide Corporation.

‡This author is on sabbatical leave from and supported in part by the University of Alabama, Birmingham, Al. 35294.

¹J. E. Wertz, P. Auzins, J. H. E. Giffiths, and J. W. Orton, *Disc. Faraday Soc.* **28**, 136 (1959).

²Y. Chen, M. M. Abraham, L. C. Templeton, and W. P. Unruh, *Phys. Rev. B* **11**, 881 (1975).

³Y. Chen and M. M. Abraham, *New Physics (Korean Phys. Soc.)* **15**, 47 (1975).

⁴W. P. Unruh, Y. Chen, and M. M. Abraham, *Phys. Rev. Lett.* **30**, 446 (1973).

⁵M. M. Abraham, Y. Chen, and W. P. Unruh, *Phys. Rev. B* **9**, 1842 (1974).

⁶L. E. Halliburton, L. A. Kappers, D. L. Cowan, F. Dravnieks, and J. E. Wertz, *Phys. Rev. Lett.* **30**, 607 (1973).

⁷L. E. Halliburton, D. L. Cowan, W. B. J. Blake, and J. E. Wertz, *Phys. Rev. B* **8**, 1610 (1973).

⁸M. M. Abraham, Y. Chen, L. A. Boatner, and R. W. Reynolds, *Solid State Commun.* **16**, 1209 (1975) and

references cited therein.

⁹J. W. Culvahouse, L. V. Holroyd, and J. L. Kolopus, *Phys. Rev.* **140**, 1181 (1965).

¹⁰J. T. Suss, Thesis (Hebrew University, Jerusalem, 1966) (unpublished).

¹¹A. J. Tench and M. J. Duck, *J. Phys. C* **8**, 257 (1975).

¹²M. M. Abraham, Y. Chen, and J. Rubio O., *Phys. Rev. B* **14**, 2603 (1976).

¹³M. M. Abraham, C. T. Butler, and Y. Chen, *J. Chem. Phys.* **55**, 3752 (1971).

¹⁴W. P. Unruh, Y. Chen, and M. M. Abraham, *J. Chem. Phys.* **59**, 3284 (1973).

¹⁵R. C. Duvarney and A. K. Garrison, *Solid State Commun.* **12**, 1235 (1973).

¹⁶A. Abragam and B. Bleaney, *Electron Paramagnetic Resonance of Transition Ions* (Oxford U.P., London, 1970), p. 508.

¹⁷G. Rius and R. T. Cox, *Phys. Lett. A* **27**, 76 (1968).

¹⁸G. Rius, R. T. Cox, P. Freund, and J. Owen, *J. Phys. C* **7**, 581 (1974).

¹⁹P. McGeehin, B. Henderson, J. F. Boas, and T. P. P. Hall, *J. Phys. C* **8**, 1718 (1975).

²⁰H. Bill and R. Lacroix, *Phys. Lett.* **21**, 257 (1966).